DOI: 10.17277/amt.2019.01.pp.035-044

C–V (*g–V*) Characteristics of M–$Ba_xSr_{1-x}TiO_3$–M Thin Film Structures with Oxygen Vacancies

V. Buniatyan*, V. Begoyan, A. Davtyan, H. Hovnikyan, P. Avetisyan

National Polytechnic University of Armenia (*NPUA*),
105 Teryan St, 0009, Yerevan, Armenia

***** Corresponding author Tel. +3749 131 16 39. *E-mail*: vbuniat@seua.am, vbuniat@yahoo.com

Abstract

The paper studies the *C–V* (*g–V*) characteristics of thin film metal-ferroelectric-metal (*m-f-m*) structure, with a ferroelectric-paraelectric phase and high concentration of oxygen vacancies in the interfacial regions of metal-ferroelectric contacts. It is assumed that these vacancies create electron trap levels in the band gap of the ferroelectric. The nonlinear dependence of permittivity on applied electric field is taken into account. It is assumed that with an increase in the applied electric field the oxygen vacancies conditioned trap levels are ionize due to de-trapping of electrons via Pool–Frenkel emission. Based on these assumptions analytical expressions were derived for *C–V*, *g–V* dependencies and bias dependent loss tangent. All dependencies were in good agreement with the experimental results.

Keywords

Ferroelectric; trapping/de-trappinglevel; Pool–Frenkel emission.

Introduction

Over the past 20 years, ferroelectric thin films have been of a considerable interest, driven by the possibility of their application in non-volatile memory, micro-electromechanical systems (**MEMS**), ferro-electric FETs, solid-oxide fuel cells (**SOFC**), etc. [1 – 6]. Particularly, thin-film varactors utilizing field-dependent permittivity ("tunability") ferroelectrics have attracted considerable attention for a wide range of phase and frequency agile microwave devices. For tunable microwave application low microwave losses, low leakage currents and high tenability are the main advantages of perovskite $Ba_xSr_{1-x}TiO_3$ (**BST**) over other ferroelectric compositions [2 – 5]. Derived mainly by this application of the *C–V* (*C–T*), *g–V* (*g–T*) dependencies, losses mechanisms as well as the experimental hysteresis effects in thin BST film-based devices have been subjects of extensive studies [1 – 6]. The main objective of this research is the analysis and interpretation of the experimental results including impact of the defects on the performances of the devices. We consider the negative impact of the structural defects, impurities and quality of interfaces on the device performance. The research showed that the shape of the *C–V* (*C–T*), *g–V* (*g–T*) curves strongly depends on the conduction mechanisms (SCL, Schottky, Tunnel, Fowler-Nordheim, Pool-Frenkel, etc.) and on the presence of oxygen vacancies (as the inevitable defects in ferroelectric materials), nature and density of the interface states, traps and etc. [1 – 3, 7 – 10, 11]. It was shown experimentally, that in agile microwave devices, based on paraelectric phase ferroelectrics, the oxygen vacancies cause high RFand DC leakages currents, microwave losses and distortion (hysteresis) of *C–V*, *g–V*, tanδ–*V*, and I–V dependences. In memory applications, the oxygen vacancies cause fatigue [2 – 4]. To the best of the authors' knowledge, there are relatively very few studies where the electro-physical processes, such as nonlinearity of permittivity, trapping/de-trapping of charge carriers by oxygen vacancies are involved for modeling *C–V*, *g–V* dependencies and hysteresis.

In this paper, we offer new approaches to derive analytical expressions for the above mentioned *C–V*, *g–V* dependencies, which, in turn, allow for easy modeling of these characteristics and explicit interpretation of all experimental results, obtained by different authors.

Physical model

The present study is based on following assumptions:

(i) oxygen vacancies concentration is very high especially at the interfaces with the electrodes and acts as donors, which cause the *n*-type conductivity, while internal low vacancies region (core) have the *p*-type semiconductor properties [1, 5, 12 – 14]. Currently, it is well established that the oxygen vacancies play a major role. The oxygen concentration is not constant throughout the film. It decreases sharply near the metal electrodes, approximately 50 % of its value in the center (≈20 nm from the Pt surface) [16] (Fig. 1). At sufficiently high temperatures or high fields, the oxygen vacancies are double ionized, each supplying two electrons to the conduction band according to reaction

$$O_0 \leftrightarrow \frac{1}{2}O_2(\text{gas}) + V_0^{"} + 2e^{-}.$$

An interstitial oxygen atom can form different types of defects $x = O^0, O^-, O^{2-}$, which means that the triplet states of oxygen correspond to three different energies in the energy band of ferroelectric film. Investigation of the electrical and optical properties of deep-level $SrTiO_3$ [1, 12 – 15] thin film grown by organometallic chemical-vapour deposition show that dominant defects in the $SrTiO_3$ consisted of a series of deep-level trapping states with energies in the range of E_v + 2.4 eV to E_v + 3.15 eV and a series of shallower traps near the conduction-band edge in the range of $E_c - E_{tn}$ = (0.06–0.4) eV. These dominant electron traps were attributed to oxygen vacancy or iron transition–metal/oxygen vacancy defects. The defect concentration ranges from 10^{14} to 10^{18} cm^3 in the films. Even this concentration was estimated (10^{20}–10^{22}) cm^3 [1, 2, 12 – 15]. This process can be described as follows: the oxygen vacancies act as donors, which cause the *n*-type conductivity (Fig. 2). The non-uniform distribution of the oxygen vacancies near the interfaces causes bending of the energy bands and changes the shape of the barrier (Fig. 3), making it for charges easier to overcome. On the other hand, the experimentally observed leakage currents may be explained by conductivity associated with the oxygen vacancies [1, 2, 5]. The oxygen vacancies are the most mobile in perovskite ferroelectrics [1 – 3, 9, 11]. The experimental results of both mono-crystalline and polycrystalline BSTO at high temperatures [15] showed that the conductivity of undoped polycrystalline titanate oxides depends on oxygen partial pressure of the ambient gas. Since the interface with electrodes is poor with O^{2-}, these interfacial layers have the *n*-type, while internal region is *p*-type with local *n*–type regions. In the neutral state, the donor level is double occupied, and there is a reduced repulsive interaction between the vacancy and neigh-boring cations. The interfacial vacancies cause distortion of the crystal lattice and polarization fields around the vacancy. This makes the levels deeper and causes them to act as charge traps [1, 12, 13, 15]. The interfacial built-in electric fields associated with the trapping centers and oxygen vacancies result in changes the interfacial permittivity of the films [15]. It is worthwhile to notice that the oxygen vacancies are not to be only main defect of ferroelectric films [1, 5, 12 – 14]. The Ba, Sr vacancies in BSTO result in shallow acceptor levels. Dopants also result in levels in the forbidden band. N_b gives a shallow level, while Mn, Gr, and Fe give levels near the midgap. Pt gives a deep level also near the midgap [1, 11 – 15];

(ii) Under the applied DC field, the traps release electrons via Poole–Frenkel mechanism and become charged. Due to the change of oxygen vacancies "conditioned" trapped deep electrons occupation (distribution, *f(V)*) function in films (ceramics) are formed, including a new high electric polarized field.

The eclectic field of a point charge polarizes the crystal locally, reducing its permittivity which in turn brings to hysteresis behaviour in *C*(*V*), and dielectric constant, ⊥(*V*), as well as can be influence of *I*(*V*) dependence[2, 15];

(iii) The dielectric permittivity of ferroelectric materials is nonlinear dependence of applied electric field $\varepsilon(E,r) = \varepsilon(0)\left(1 + AE^2\right)^{-1}$, where $A = 3\beta[\varepsilon_0\varepsilon(0)]^3$, and $\varepsilon(0)$ is the permittivity at zero bias, ε_0 is the vacuum dielectric constant. For example, for $SrTiO_3$, $\beta = 8 \cdot 10^9$ V·m^5/C^3, $\varepsilon(0) = 106$, and $A = 0.45 \cdot 10^{-15}$ (m/V)^2 [1, 2, 5].

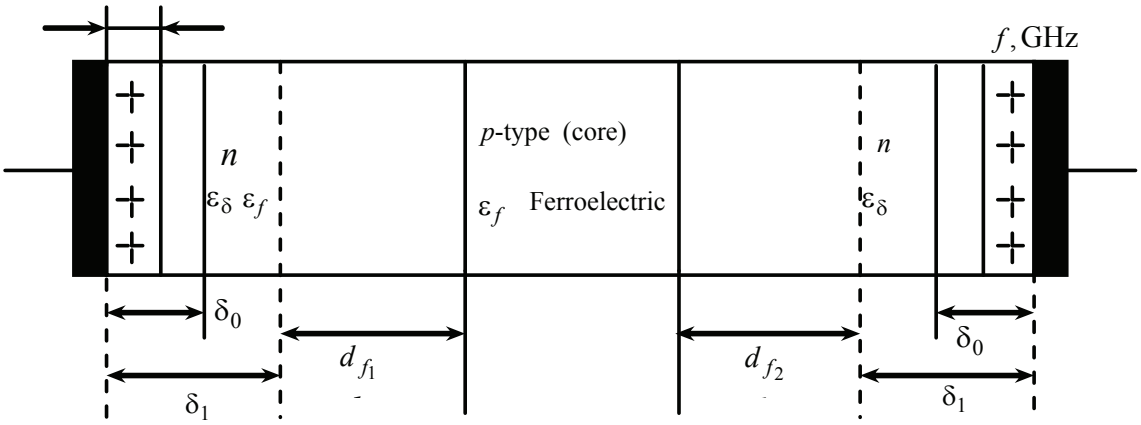

Fig. 1. Cross-section of *p*-type ferroelectric with a local *n*-type region associated with oxygen vacancies

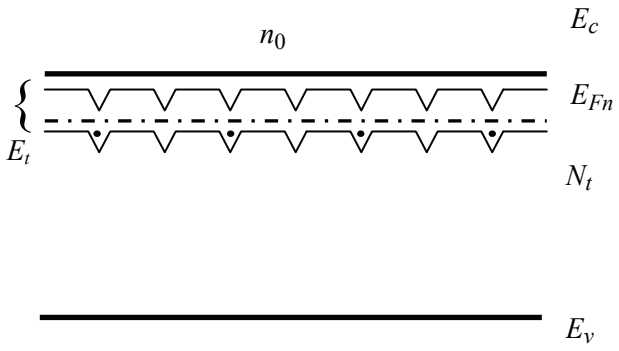

Fig. 2. Schematics of trap levels (one-dimensional) for electrons

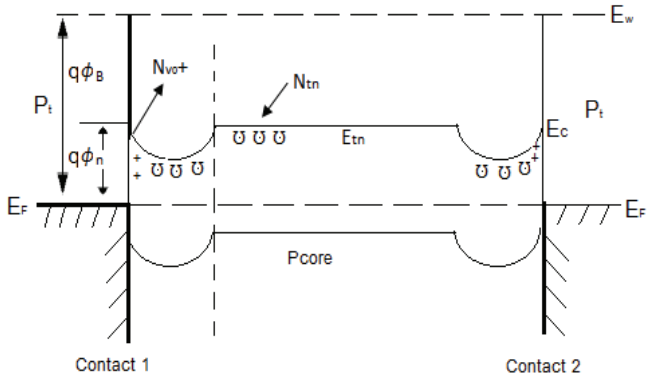

Fig. 3. Schematics of band diagram of *m-f-m* structure

Theory and model description

Let us consider the Pt–$B_xS_{1-x}TiO_3$–Au structure (Fig. 1, Fig. 3). It is well known, that for the measure of *C–V* (*C–f*) characteristics of *m-f-m* structure it is necessary to apply dc voltage, U_0, and simultaneously, small signal ac voltage, U_{1m}, where $|U_{1m}| << U_0$. We assume that before DC field is applied on BST film, the concentration of free electrons n_{c0} is quite low, of the band of ferroelectrics and the electrical activity of charged oxygen vacancies is compensated by the trapped electrons or corresponding ionized acceptors connected, for instance, with the film non-stoichiometry [1, 5, 15]. It means, that the relation between free and captured carriers changes because of the small injection from the Schottky barrier and due to de-trapping of electrons via Pool–Frenkel emission [1, 2, 5, 7, 9, 10, 15] from the oxygen vacancies originated trap levels to the conductance band of ferroelectric.

Let the concentration of oxygen vacancies near the metal contact be N_t, which act as "donors" and its average depth in respect of the edge of the ferroelectric conductance band (E_c) be E_t (Fig. 2), as well as that the free electron concentration distribution correspond to the Fermi–Dirac function, i.e.

$$n = n_i + n_{pF} + n_0 \cong N_c \exp\left(\frac{F - E_c}{kT}\right), \qquad (1)$$

where n_0 is the free electron concentration in equilibrium condition, n_i is the concentration of injected electrons, n_{pF} the concentration of electrons realized via Pool–Frenkel emission, F is the imref, E_c is the conductance band bottom energy, k is the Boltzmann's constant, T is the absolute temperature, N_c is the density of the states in conduction band. The concentration of trapped electrons given by [17 – 19]:

$$n_t = \frac{N_t}{1 + \frac{1}{g}\exp\left(\frac{E_t - F}{KT}\right)} = \frac{N_t}{1 + \gamma(E_t)/n}, \qquad (2)$$

where $\gamma(E_t) = \frac{N_c}{g}\exp\left(\frac{E_t - F}{KT}\right)$ is the Shockley–Read stat factor, g is the degeneracy factor and equal to 2 for

electrons becomes of the fact that a donor level can accept one electron with either spin or can have no electron.

If the trap capture rate is $S_n = \langle V_{th}\sigma \rangle$ (where V_{th} is the thermal velocity of electrons, is capture cross section) then the thermal and Pool–Frenkel ionizations probabilities of traps are P_e and P_F, respectively, the free electron concentration in conductance band is n, the concentration of trapped electrons is n_t, for the trapped electron concentration kinetic equation will have the form:

$$\frac{\partial n_t}{\partial t} = S_n(N_t - n_t)\, n - (P_e + P_F)\, n_t . \qquad (3)$$

When studying the small-signal characteristics of *m-f-m* structures as described below, the interfaces of *m-f* regions are looked upon as the high concentration of oxygen vacancies and the central region (core) of ferroelectric film is assumed as a *p*-type semiconductor properties layer (see Fig. 1), and the existence of vacancies creates trap levels for electrons.

For the small-signal analysis (harmonic approximation), the parameters are usually set as a sum of constant and small variable components, like:

$$U = U_0 + U_1 = U_0 + U_{1m}\, e^{i\omega t}, \quad |U_{1m}| << U_0;$$

$$n = n_0 + n_{1m}\, e^{i\omega t}, \quad |n_{1m}| << n_0;$$

$$\varepsilon = \varepsilon_0 + \varepsilon_{1m}\, e^{i\omega t}, \quad |\varepsilon_{1m}| << \varepsilon_0;$$

$$n_t = n_{t0} + n_{t1m}\, e^{i\omega t}, \quad |n_{t1m}| << n_{t0}$$

and etc.

When external DC field is applied and its magnitude is increased, the part of oxygen vacancies is ionized additionally due to de-trapping via Pool-Frenkeleffect. At the equilibrium condition $\frac{\partial n_t}{\partial t} = 0$, and $S_n(N_t - n_{t0})n_0 = n_{t0}P_0$ where $n_0, n_{t0}, \; P_0 = P_e + P_F$, there are free trapped concentrations of electron and its ionization probabilities at thermal equilibrium condition, respectively. From Eq. (1) and Eq. (3) we have:

$$P_0 = S_n \gamma(E_t).$$

For the alternating components of (2) we can find:

$$[i\omega + S_n(\gamma + n_0)]\, n_{t1m} = n_{1m} S_n \frac{\gamma N_t}{\gamma + n_0}; \qquad (4)$$

$$n_{t1m} = \frac{n_{1m} S_n \gamma N_t [S_n(\gamma + n_0) - i\,\omega]}{(\gamma + n_0)\left[S_n^2(\gamma + n_0)^2 - \omega^2\right]}; \qquad (5)$$

$$n_{t1m} = \frac{n_{1m} S_n^2 \gamma N_t (b_1 - i\,\omega)}{b_1\left(b_1^2 + \omega^2\right)},$$

$$b_1 = S_n(\gamma + n_0), \;\; \gamma + n_0 = \frac{b_1}{S_n}, \qquad (6)$$

where n_{1m} and n_{t1m} are the alternating components of free and captured electron concentration in the conductance band and traps, respectively, due to injection, trapping and DC-trapping processes.

On the other hand, taking into account that dielectric permittivity of ferroelectric film is nonlinear dependence from electric field as in [1, 2, 5, 15]:

$$\varepsilon(E_0) = \frac{\varepsilon_0 \varepsilon(0)}{1 + A\, E_0^{\,2}} = \frac{\varepsilon_\Gamma}{\beta} >> \varepsilon_{1m},$$

where $A = 0.45 \cdot 10^{-11} \frac{\text{cm}^2}{\text{V}^2}$, $\varepsilon_0 = 8.85 \cdot 10^{-14}$ F/cm, $\varepsilon(0)$ is the permittivity at zero electric field, (for example, for $SrTiO_3$ $\varepsilon(0) \cong 106$, $\beta = 1 + A E_0^{\,2}$, and ε_{1m} is the alternating component of permittivity.

The second peculiarity of the present treatment is as follows: we assume that $\tau_t << \omega^{-1}$, i.e. the transit time of electrons, τ_t, through to the film is small in compare of measure signal frequency ω^{-1}. In this conditions it is valid to use the theory, developed in [20], according to which $(n_{t1m} + n_{1m})$ can be presented as:

$$(n_{t1m} + n_{1m}) = A_0 U_1 A_0 = \frac{\partial(n_0 + n_{t0})}{\partial U_0}. \qquad (7)$$

Substituting the n_{1m} from (6) into (7), we have:

$$n_{1m} = \frac{A_0 U_1 b_1 \left(b_1^2 + \omega^2\right)\left(b_2 + i\,\omega S_n^2 \gamma N_t\right)}{b_2^2 + \left(S_n^2 \gamma N_t \omega\right)^2};$$

$$n_{1m} = \left\{1 + \frac{S_n^2 \gamma N_t (b_1 - i\,\omega)}{b_1\left(b_1^2 + \omega^2\right)}\right\} = A_0 U_1;$$

$$b_2 = b_1\left[\left(b_1^2 + \omega^2\right) + S_n^2 \gamma N_t\right]. \qquad (8)$$

Neglecting the diffusion component of current for the density of total alternating current include also the displacement component, $\frac{\partial D}{\partial t} = \frac{\partial[\varepsilon(E)E]}{\partial t}$, we will have:

$$j_1 = S\left\{i\omega \frac{\varepsilon_\Gamma}{\beta} E_{1m} + q\,\mu\, E_0\, n_{1m} + q\,\mu\, E_{1m}\, n_0\right\}, \qquad (9)$$

where taking into account that $\varepsilon(E_0)=\frac{\varepsilon_0\varepsilon(0)}{1+A\cdot E_0^{\,2}}=\frac{\varepsilon_\Gamma}{\beta}>>\varepsilon_{1m}$, $\varepsilon_\Gamma=\varepsilon_0\,\varepsilon_{\rm BST}$, S is the cross section area of ferroelectric film, μ is the mobility of electrons, n_0 and n_{1m}, E_0 and E_{1m} are the constant and alternating components of free electrons and electric field, respectively,

$$j_1=\frac{S\,\varepsilon_\Gamma}{\beta}\left\{(i\,\omega+\omega_1)E_{1m}+\frac{\omega_1}{n_0}E_0\,n_{1m}\right\},$$

$$\omega_1=\frac{q\,\mu\,\beta\,n_0}{\varepsilon_\Gamma}. \qquad (10)$$

For the complex conductivity and its components we will have

$$\dot{Y}=\frac{S\,\varepsilon_\Gamma}{\beta\,l}\{i\,\omega(C_0+C_t)+g_0+g_t\}, \qquad (11)$$

where

$$C_0=\frac{S\,\varepsilon_\Gamma}{\beta\,l}=\frac{S\,\varepsilon_0\,\varepsilon(0)\,l^2}{\left(l^2+A\,U_0^{\,2}\right)l}=\frac{S\,\varepsilon_\Gamma\,l}{l^2+A\,U_0^{\,2}};$$

$$C_t=\frac{2S\,\varepsilon_\Gamma\,\mu\,b_1\,U_0\left(b_1^{\,2}+\omega^2\right)\left(l^2-A\,U_0^{\,2}\right)S_n^{\,2}\gamma\,N_t}{l\left(l^2+A\,U_0^{\,2}\right)^2\left[b_2^{\,2}+b_3^{\,2}\right]};$$

$$g_0=\frac{S\,q\,\mu\,n_0}{l};$$

$$g_t=\frac{2S\,\varepsilon_\Gamma\,\mu\left(l^2-A\,U_0^{\,2}\right)b_2\,b_1\left(b_1^{\,2}+\omega^2\right)U_0}{l\left(l^2+A\,U_0^{\,2}\right)^2\left[b_2^{\,2}+b_3^{\,2}\right]};$$

$$b_3=\omega\,S_n^{\,2}\,\gamma\,N_t;$$

$$\mathrm{tg}\delta=\frac{10^{-6}(g_0+g_t)}{6.28\,f_1(C_0+C_t)},$$

C_0 is the geometrical capacitance and dc conductance of *m-f-m* structure, l is the length of ferroelectric film, U_0 is the applied DC voltage, n_0 is the free electron concentration (include SCL, Schottky injection and Pool-Frenkel emission), C_t and g_t are the so called "trapping" dynamic capacitance and conductivity, respectively, which are conditioned by Pool-Frenkel mechanism ionization processes. As it follows from the expressions of C_t and g_t, they both depend on applied alternating signal frequency, ω, as well as strongly depend on concentration of oxygen vacancies and its energy distribution via the parameters of b_1, b_2, b_3. The equivalent circuit of the *m-f-m* structure neglecting the metallic plane and contact pads parasitic capacitances and inductances, can be presented as in Fig. 4 [2, 3], where there are separated the geometric capacitance, C_0 and electronic conductance g_0, in respect of the trap levels conditioned corresponding values of C_t and g_t in order to understand the physical processes which occur in traps as well as for explicit explanation of the dependences of parameters and their comparison with the experimental results. Neglecting the r_{cb} and L_c, for the simple equivalent scheme we will have (Fig. 5).

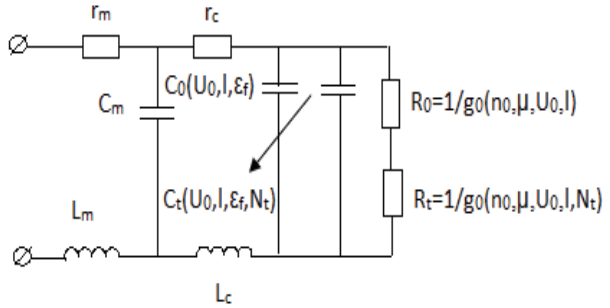

Fig. 4. Equivalent circuit of the *m-f-m* structure
(r_m, C_m and L_m are the interconnection (pads) are the metallic plate resistance and inductance)

Numerical calculations and their comparison with the experiments

The numerical calculations were carried out according to Eq. (11) for the follow parameters of ferroelectric BST films and output signal parameters:

$$f=10^6\div10^{11}\ \text{Hz},\quad n_0=10^{10}\div10^{13}\ \text{cm}^{-3},$$
$$N_t=10^{16}\div10^{19}\ \text{cm}^{-3},\quad S=7\cdot10^{-6}\ \text{cm}^2,$$
$$l=100\div600\ \text{nm},\quad \mu=0.01\div30\ \frac{\text{cm}^2}{\text{V}\cdot\text{s}},$$
$$\varepsilon_\Gamma=8.85\cdot10^{-14}\varepsilon(0)_{\rm BST},\quad U_0=-20\div+20\ \text{V},$$
$$\sigma=10^{-14}\div10^{-16}\ \text{cm}^2,\quad N_c\approx10^{17}\ \text{cm}^{-3},$$

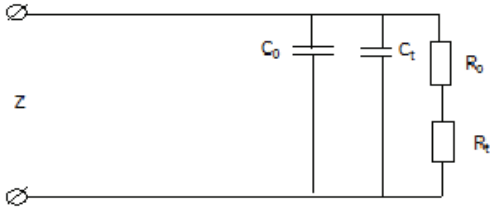

Fig. 5. Simplified equivalent circuit of *m-f-m* structure resistance, capacitance and inductance, and r_m, L_m

$$g = 2,\ S_n = \sigma\langle V_{th}\rangle,\quad V_{th} \approx 10^7\ \text{cm/s},$$
$$\Delta E_t = 0.06 \div 0.4\ \text{eV},\quad \varepsilon(0) \cong 106.$$

The values of these parameters were taken from the experimentally investigated real structures carried out in [2, 3, 21 – 23] and many other authors [1, 5, 24, 25].

The results of theoretical calculations and experimental investigations of *m-BST-m* structures are presented in Fig. 6 – 10. For comparison of theoretical and experimental dates, we have used the results of investigations carried out in [21 – 25]. In Fig. 6*a–c* is presented the experimental research results of the thin test varactors, which are fabricated by RF magnetic sputtering using a $Ba_{0.5}Sr_{0.5}TiO_3$ target (prepared in NPUA) and tested in Chalmers Technological University (Sweden) [2, 21 – 23]. The films are 290 – 560 nm thick.

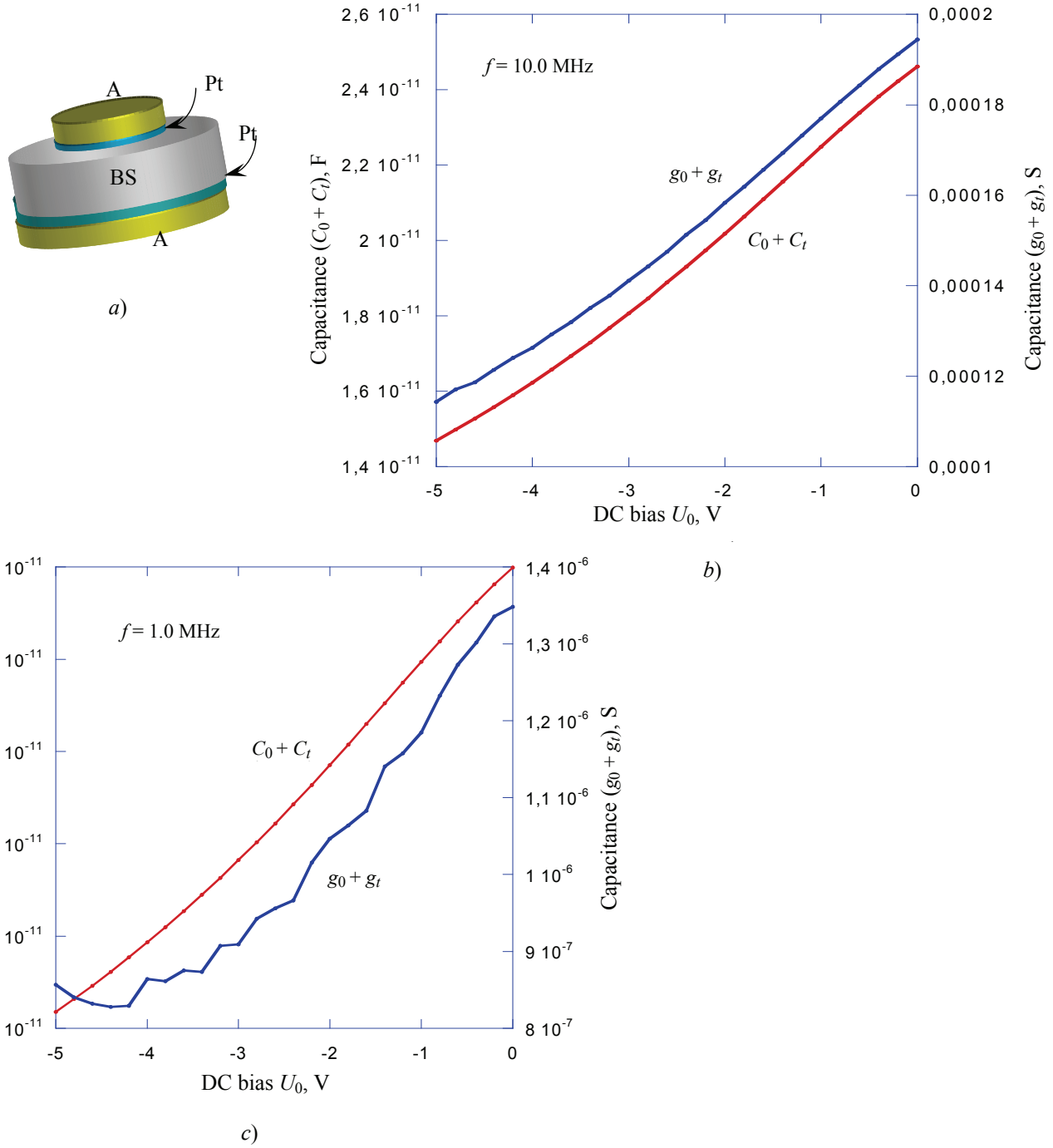

Fig. 6. Structure of the test varactor $Ba_{0.25}Sr_{0.75}TiO_3$ (*a*), DC bias dependent capacitance and conductance measured at 1.0 MHz (*b*) and 10.0 MHz at room temperature (*c*), area $S = 7 \times 10^{-6}$ cm^2, $l = 290$ nm

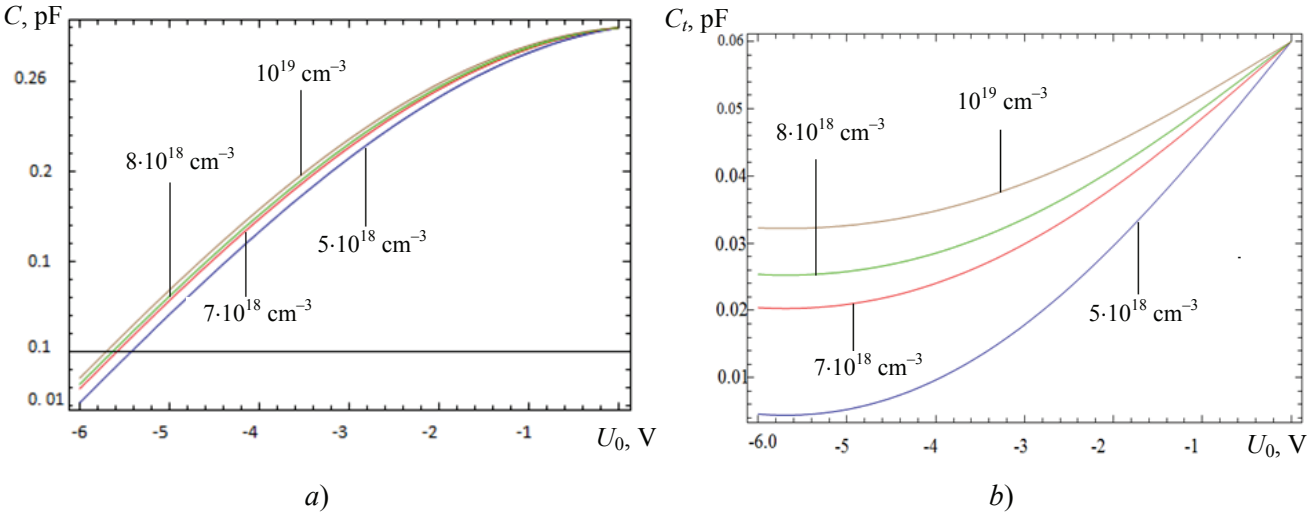

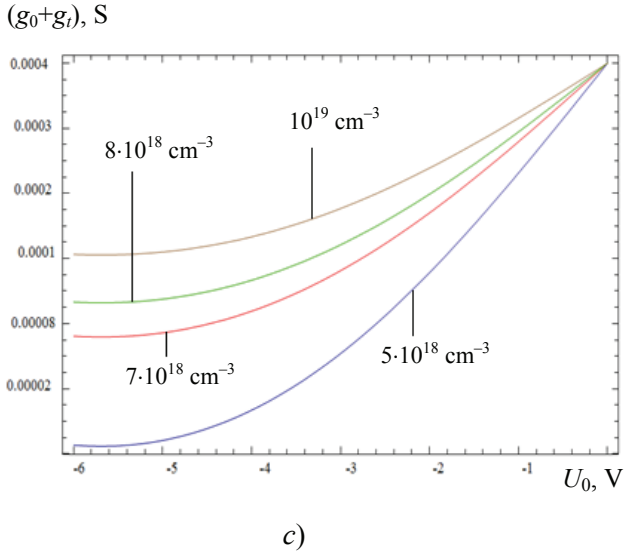

← **Fig. 7. Theoretical (calculated) dependences of C–U_0 (*a*), C_t–U_0 (*b*), g–U_0 (*c*) ($C = C_0 + C_t$, $g = g_0 + g_t$) for different values of trap concentration, N_t, according to (11) and for the follow parameters of $Ba_{0.25}Sr_{0.75}TiO_3$ films:** $E_t = 0.26$ eV; $\mu = 30$ cm^2/Vs, $f = 1.0$ MHz; $\sigma = 10^{-14}$ cm^2, area $S = 7 \times 10^6$ cm^2, $l = 290$ nm, $n_0 = 10^{11}$ cm^{-3}

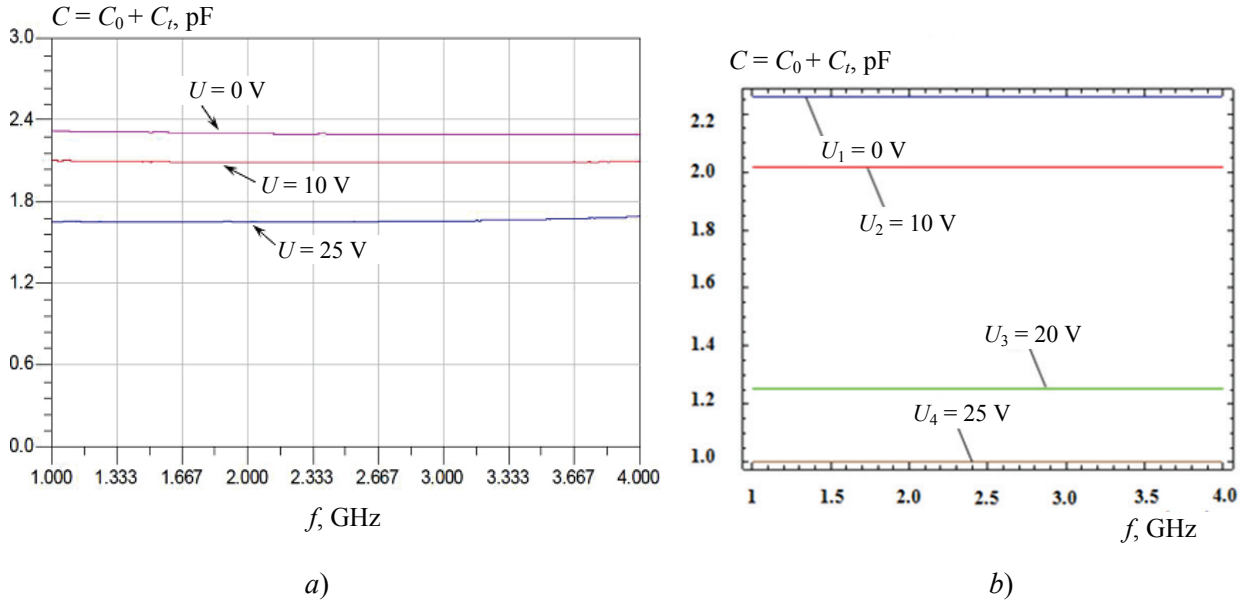

Fig. 8. Experimental (*a*) and theoretical (*b*) dependencies of $C = C_0 + C_t$ on signal frequency, f, for the different values of applied voltage U_0 of $Ba_{0.25}Sr_{0.75}TiO_3$ based voltage tunable capacitors [2, 21 – 23].
The other parameters are: $E_t = 0.26$ eV, $N_t = 10^{19}$ cm^{-3}, $\mu = 30$ cm^2/Vs, $l = 290$ nm, $n_0 = 10^{11}$ cm^{-3}, $\varepsilon(0) = 106$ (STO), $\sigma = 10^{-14}$ cm^2, area $S = 7 \times 10^6$ cm^2

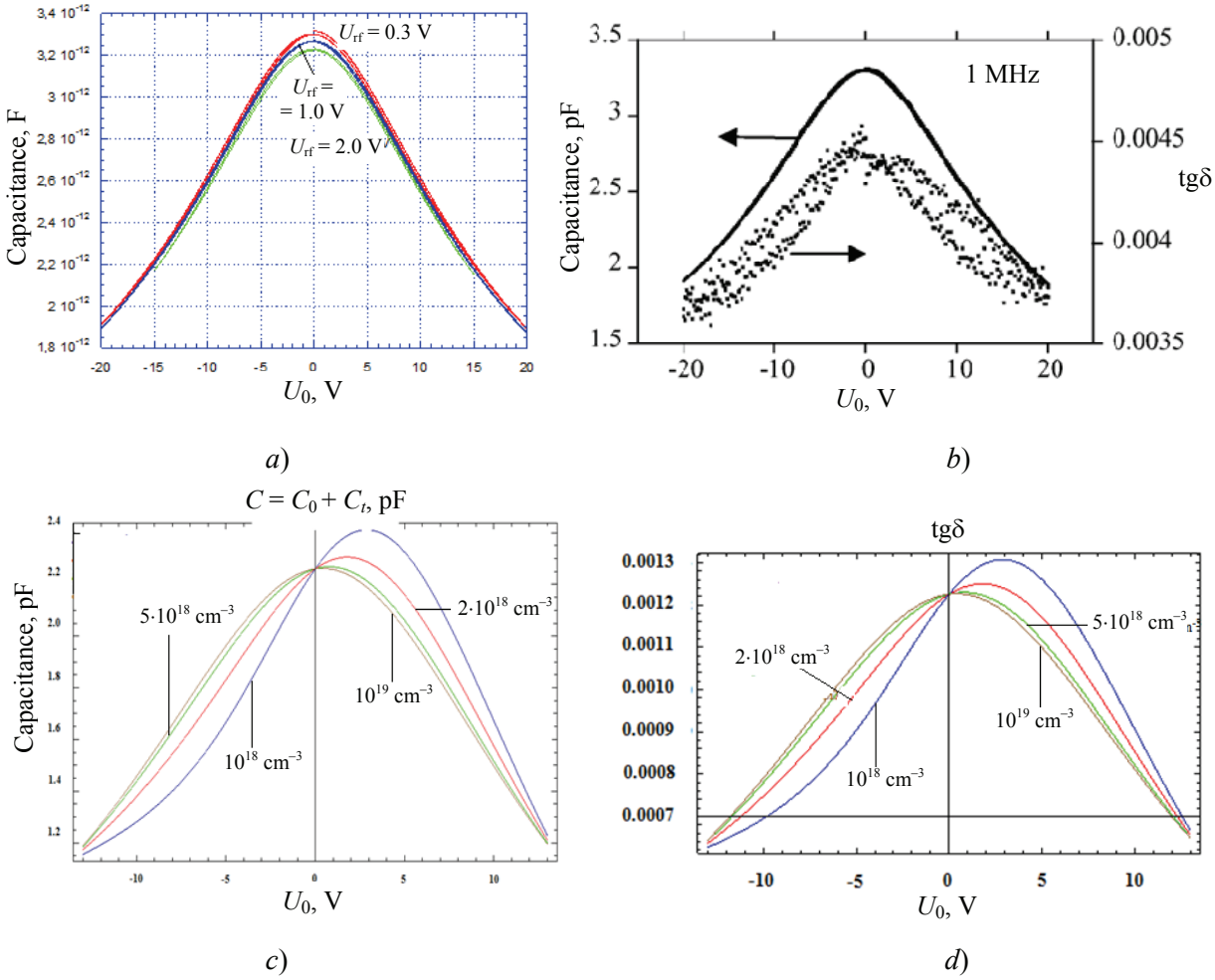

Fig. 9. Experimental dependencies of test varactor (Fig. 6 *a*, *b*) capacitance and tanδ, on applied voltage, U_0, measured at different U_{rf} voltages and theoretical calculated dependencies (*c*, *d*) of $C = C_0 + C_t$ and tanδon applied voltage, U_0, for different values of trap concentration, N_t. signal frequency f = 1.0 MHz.

The other parameters are: E_t = 0.26 eV, μ = 30 cm^2/Vs, l = 290 nm, $n_0 = 10^{11}$ cm^{-3}, ⊥(0) = 106 (BST), σ = 10^{-14} cm^2, area, $S = 7 \times 10^{-6}$ cm^2

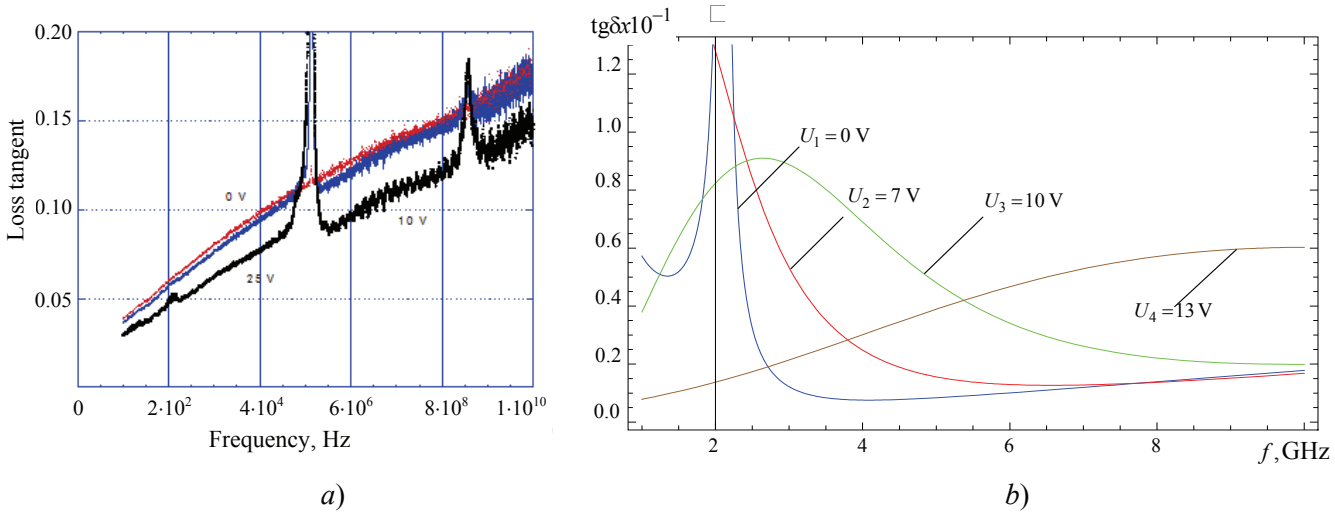

Fig. 10. Experimental (*a*) [2, 21 – 23] and theoretical dependencies of tgδ (*b*) on signal frequency f for the different values of applied voltage U_0

(The other parameters are as in Fig. 9)

Fig. 7 presents the theoretical calculations of $C–U_0$, $C_t–U_0$, $g–U_0$, $(C = C_0 + C_t,\ g = g_0 + g_t)$ dependencies according to (11) for above mentioned parameters of the BST film. Figure 8 – 10 depict the experimental and theoretical dependencies of $C = C_0 + C_t$ on signal frequency, dependencies of test varactor (Fig. 6*a*, *b*) capacitance and tanδ, on applied voltage, U_0, for different values of trap concentration, N_t, etc.

Conclusions

As it follows from expression (11), for the first approximation, the "trapped" capacitance is forward and the "trapping" conductance is reverse proportional to oxygen vacancy's conditioned trap concentration, N_t, and in complex form depend on parameter, $\gamma(E_t)$, that is energy depth of trap levels, E_t, depend on capture cross section of traps, $S_n = \sigma V_{th}$, signal frequency, ω, as well as depend on geometrical and material parameters of ferroelectric thin films, such as: coefficient *A*, length, *l*, cross section area, *S*, dielectric permittivity, ε_Γ, and applied signal parameters, U_0. The geometrical capacitance of structure, C_0, will decrease with the increase of applied field, U_0, and the constant component of the geometrical conductance, g_0, is forward proportional to the free concentration of electrons and its mobility. It is follows from (11) expression also, that as small the value of E_t, are higher of free electrons concentration and conductance, for the all other equal conditions. Moreover, in this conditions the "trapped" capacitance will be decrease with the increase E_t, because of decrease of the trapped electron concentration. Comparison of experimental and calculated results, presented in Fig's 6 – 10 shows that theory and experiments are qualitatively agree each to other. Thus we can conclude that for design, mathematical modeling, characterization and theoretical calculations of the $A_{1-x}A_x'BO_{3-b}$ thin-film based active and passive devices/sensors parameters, as well as for interpretation of the experimental results in these fields, it is necessary to create new physical mathematical concepts and modelling methods of characterization of above mentioned parameters and take into account the following:

i) the presence of oxygen vacancies as a most mobile and abundant defects in perovskite ferroelectrics;

ii) the dielectric permittivity of ferroelectric materials is nonlinear dependence of applied electric field;

iii) under applied DC field the traps release electrons via Poole-Frenkel mechanism and become charged.

The results will contribute to a better understanding of electro-physical processes which take place in $A_{1-x}A_x'BO_{3-b}$ real nano-film based devices. We anticipate that the new knowledge that emerges from this study will provide the basis for the development of new analytical dependencies and on its base new CAD modeling procedures for optimize the polarization, hysteresis, fatigue and other properties of $A_{1-x}A_x'BO_{3-b}$ real nano-film based devices as well as to more precise explanation of the experimental results in these fields.

References

1. Dawber M., Raba J.F., Scott J.F. Physics of thin-film ferroelectric oxides. *Rev. of Modern Phys*., 2005, vol. 77, pp. 1083-1130.

2. Gevorgian S.Sh. *Ferroelectrics in Microwave Devices, Circuits and Systems*.Springer-Verlag, London, 2009, 394 p.

3. Gevorgian S.Sh., Tagantsev A.K., Vorobiev A.K. *Tunable Film Bulk Acoustic Wave Resonators*. Springer-Verlag, London, 2013, 243 p.

4. Meyers C.J.G., Freeze C.R., S.Stemmer, et al. $(Ba,Sr)TiO_3$ tunable capacitors with RF commutation quality factors exceeding 6000. *Appl. Physics Lett.*, 2016, vol. 109, p. 112902.

5. Tagantsev A.K., Sherman V.O., Astafiev K.F. et al. Ferroelectric Materials for Microwave Tunable applications. *Journal of Electroceramics*, 2003, vol. 11, pp. 11-66.

6. York R.A. Tunable Dielectrics for RF Circuits. In *Multifunctional Adaptive Microwave Circuits and Systems*, edited by M. Steer and W. D. Palmer (Sci Tech Publishing), 2009.

7. Pintilie L., Boerasu I., Gomes M.J.M., et al. Metal-ferroelecric-metal structures with Schottky contacts. Analysis of the experimental current-voltage and capacitance-voltage characteristics of $Pb(Zn, Ti)O_3$ thin films. *Journal of Applied Physics*, 2005, vol. 98, pp. 124104-124104.

8. Wang Y.-P., Tseng T.-Y. Electronic defect and trap-related current of $(Ba_{0.4}Sr_{0.6})$ $Ti0_3$ thin films. *Journal of Applied Physics*, 1997, vol. 81, issue 10, pp. 6762-6766.

9. Wang R.-V., Mclntyre P.C. Point defect distributions and their electrical effects on (Ba,Sr)TiO/Pt thin films. *Journal of Applied Physics*, 2003, vol. 94, issue 3, pp. 1926-1932.

10. Mitrofanov O., Manfa and M. Pool-Frenkel electron emission from the traps in AlGaN/GaN transistors. *Journal of Applied Physics*, 2004, vol. 95, pp. 6414-6419.

11. Boikov Yu.A., Goltsman B.M., Yarmarkin V.K. et al. Slow capacitance relaxation in (BaSr)TiO_3 thin films due to the oxygen vacancy redistribution. *Appl. Phys. Lett.,* 2001, vol.78, issue 24, pp. 3866-3868.

12. Robertson J. Energy levels of point defects in Ba(Sr)TiO_3 and related oxides, *Journal of Applied Physics*, 2003, vol. 93, issue 2, pp. 1054-1059.

13. Robertson J. Interfaces and defects of high-K oxides on silicon. *Solid state Electronics*, 2005, vol. 49, pp. 283-293.

14. Park C.H., Chadi D.J. Microscopic study of oxygen-vacancy defects in ferroelectric perovskites. *Phys. Rev. B*, 1998, vol. 57, issue 22, pp. 13961-13964.

15. Buniatyan V., Martirosyan N., Vorobiev A. et al. Dielectric model of point charge defects in insulating paraelectric perovskites. *Journal of Applied Physics*, 2011, vol. 110, pp. 094110-1-11.

16. Gerblinger J., Meixner H. Electrical conductivity of sputtered films of strontium titanate. *Journal of Applied Physics*, 1990, vol. 67, pp. 7453-7459.

17. Sze S.M., Kwok K.Ng. *Physics of Semiconductor Devices*. A John Wiley & Sons, Inc., Publ., 2007, 816 p.

18. Lampert M.A., Mark P. *Current Injection in Solids*. Acad. Press New-York and London, 1970, 416 p.

19. Milnes A.G. *Deep Impurities in Semiconductors*. John Wiley & Sons, New-York, 1977, 546 p.

20. Musabekov T.Y., Sandomirski V. B. *Problemi plyonochnoy elektroniki* [*Problems of thin-film electronics*]. Sov. Radio Publ., 1966. 288 p. (Rus)

21. Vorobiev A., Rundqvist P., Khamchane K., et al. Microwave loss mechanisms in $Ba_{0.25}Si_{0.75}TiO_3$ films. *Journal of Applied Physics*, 2004, vol. 96, pp. 4642-4649.

22. Vorobiev A., Rundqvista P., Gevorgian S. Microwave loss mechanisms in $Ba_{0.25}Sr_{0.75}TiO_3$ films. *Materials Science and Engineering B118*, 2005, pp. 214-218.

23. Vorobiev A., Berge J., Gevorgian S. Thin film $Ba_{0.25}Sr_{0.75}TiO_3$ voltage tunable capacitors on fused silica substrates for applications in microwave microelectronics. *Thin Solid Films* 515, 2007, pp. 6606-6610.

24. Astafiev K.F., Tagantsev A. K., Setter N. Quasi-Debye microwave loss as an intrinsic limitation of microwave performance of tunable components based on $SrTiO_3$ and $Ba_xSr_{1-x}TiO_3$ ferroelectrics. *Journal of Applied Physics,* 2005, vol. 97, pp. 014106-10.

25. Vendik O.G., Zubko S.P., Nikol'ski M.A. Microwave loss-factor of $Ba_xSr_{1-x}TiO_3$ as a function of temperature, biasing field, barium concentration, and frequency; *Journal of Applied Physics,*2002, vol. 92, no. 12, pp. 7448-7452.